JOURNAL OF VIROLOGY, Oct. 2000, p. 9206–9213 Vol. 74, No. 19
0022-538X/00/$04.00+0

Demyelination Determinants Map to the Spike Glycoprotein Gene of Coronavirus Mouse Hepatitis Virus

JAYASRI DAS SARMA,[1] LI FU,[1] JEAN C. TSAI,[2] SUSAN R. WEISS,[2] AND EHUD LAVI[1]*

Division of Neuropathology, Department of Pathology and Laboratory Medicine,[1] and Department of Microbiology,[2] School of Medicine, University of Pennsylvania, Philadelphia, Pennsylvania 19104

Received 19 April 2000/Accepted 20 June 2000

Demyelination is the pathologic hallmark of the human immune-mediated neurologic disease multiple sclerosis, which may be triggered or exacerbated by viral infections. Several experimental animal models have been developed to study the mechanism of virus-induced demyelination, including coronavirus mouse hepatitis virus (MHV) infection in mice. The envelope spike (S) glycoprotein of MHV contains determinants of properties essential for virus-host interactions. However, the molecular determinants of MHV-induced demyelination are still unknown. To investigate the mechanism of MHV-induced demyelination, we examined whether the S gene of MHV contains determinants of demyelination and whether demyelination is linked to viral persistence. Using targeted RNA recombination, we replaced the S gene of a demyelinating virus (MHV-A59) with the S gene of a closely related, nondemyelinating virus (MHV-2). Recombinant viruses containing an S gene derived from MHV-2 in an MHV-A59 background (Penn98-1 and Penn98-2) exhibited a persistence-positive, demyelination-negative phenotype. Thus, determinants of demyelination map to the S gene of MHV. Furthermore, viral persistence is insufficient to induce demyelination, although it may be a prerequisite for the development of demyelination.

Primary demyelination is a pathologic process in which myelin is destroyed, while neuronal axons remain relatively preserved. The demyelinating process can occur by either a direct attack on oligodendrocytes, the cells that produce and maintain myelin, or an autoimmune attack against myelin components, resulting in secondary destruction of oligodendrocytes. The most prevalent primary demyelinating disease in humans is multiple sclerosis (MS), which affects over a quarter of a million individuals in the United States (2). The etiology and pathogenesis of MS have long been investigated; however, causation has not been proven. There is a consensus that the process involves a T-cell-mediated autoimmune phenomenon that may be triggered by one or more viral infections (1). Several experimental animal models have been developed in order to better understand the mechanism of demyelination. Experimental autoimmune encephalomyelitis and several virus-induced experimental models, including coronavirus infection in mice (5), have been instrumental in providing insight into the pathogenesis of demyelination.

Coronaviruses, members of the order *Nidovirales*, form a group of enveloped single-stranded RNA viruses (22, 33, 36, 46). Many members of the nidoviruses, including coronaviruses and arteriviruses, infect the central nervous system and provide experimental animal model systems for neurologic diseases (30). The A59 and JHM strains of the murine member of the coronaviruses (mouse hepatitis virus [MHV]) produce demyelination in mice that mimics many of the pathologic features of MS (12, 15, 26, 39, 42, 46, 47). Chronic MHV-induced demyelination is immune mediated (11, 45), may be partially T-cell dependent (8), and is associated with viral persistence (25, 39) and concomitant enhancement of major histocompatibility complex class I antigens and RNA (9, 31, 32, 43, 44). However, many aspects of the mechanism of MHV-induced demyelination are still unknown.

Various biologic properties of MHV are associated with the viral envelope spike (S) glycoprotein (3, 4, 6, 10, 16, 35, 40). However, demyelination determinants in MHV have never been directly localized to any specific viral protein or gene. Direct molecular analysis and mapping of biologic properties to viral genes have been difficult because the large (31-kb) MHV genome (23, 37) is still not available in the form of a complete infectious clone amenable to genetic manipulation. The recent development of the technique of targeted RNA recombination is a useful tool for 3′-end genomic manipulations (38). This method is based on the high rate of recombination of a recipient virus (e.g., a temperature-sensitive [*ts*] mutant of A59) coinfected with a transfected plasmid containing the 3′ end of A59 and in which portions can be replaced with parallel portions of other coronaviruses. The technique of targeted recombination recently also became an important tool for studies of MHV pathogenesis (27, 28, 34, 40). Thus, to investigate whether the S gene has a significant role in controlling demyelination, we replaced the S gene of a demyelinating strain of MHV (MHV-A59) with the S gene of a nondemyelinating, closely related strain of MHV using targeted RNA recombination.

(This work was presented in part at the annual meeting of the American Society for Virology, July 1999, Amherst, Mass.)

MATERIALS AND METHODS

Viruses and cells. The following viruses were used in this study: wild-type MHV-A59 (26, 37); wild-type MHV-2 (14); and Alb4 (17), a *ts* mutant of MHV-A59 containing an 87-nucleotide deletion in the spacer B region of the nucleocapsid (N) gene. In a control virus (wtR13), described elsewhere (40), an MHV-A59 S gene was reintroduced into the genome of MHV-A59. Penn97-1 is a product of tissue culture recombination due to a dual infection with MHV-A59 and MHV-2 (J. Das Sarma et al., submitted for publication). Plaque-purified stocks of all the viruses used in this study had titers of 10^7 to 10^8 PFU/ml. Viruses were propagated and assayed in L2 and 17Cl-1 murine fibroblast cells at 37°C in Dulbecco's modified Eagle medium (GIBCO BRL, Gaithersburg, Md.) containing 10% heat-inactivated fetal bovine serum (FBS) and 1% penicillin-streptomycin in the presence of 5% CO_2. Spinner cultures of L2 cells were maintained

* Corresponding author. Mailing address: University of Pennsylvania, School of Medicine, Division of Neuropathology, Department of Pathology and Laboratory Medicine, 613 Stellar-Chance Building, Philadelphia, PA 19104-6100. Phone: (215) 898-8198. Fax: (215) 898-9969. E-mail: lavi@mail.med.upenn.edu.

TABLE 1. Primers used for introducing restriction sites into the MHV-2 S gene and for recombinant virus genome sequencing

Primer	Sequence (5′→3′)	Genome location (nucleotides)
SG1F	CTCTTCCCTAGGGTATATTGGTG	30–52 (S gene of MHV-2)
SG1R	CTTTCCTGCAGGGGCTGTGATAGTCAATCCTC	4077–4108 (3′ end of S gene and 23 bp downstream of the MHV-2 S gene stop codon)
IZJ5	GCTCCAACAGTTGGTGCC	952–696 (N gene of MHV-A59)
IZJ6	ACGTAGGACCTTGCTAACTTC	168–188 (3′ untranslated region of MHV-A59)
FIJ79	GCGAATTATAGTGGTGGCACAC	944–966 (HE gene of MHV-A59)
MHV-2S1R	GCACACAGGGGATTTTAGCTCTG	536–561 (S gene of MHV-2)
Penn11F	AAGCAGCTGAGTGACATGACCC	3287–3308 (S gene of MHV-2)
RIJ84	CCATGCATCACTCACATGCC	26–45 (ORF 5a of MHV-A59)

in Joklik's modified Eagle medium with 10% FBS at densities of between 2×10^5 and 2×10^6 cells per ml.

Plasmids. The pGEM-T$^{(a)}$ vector was purchased from Promega, Madison, Wis. The transcription vector pMH54 (obtained from Paul Masters) consists of the extension of plasmid pFV1 (7, 19) to include the 3′ 1.1 kb of the hemagglutinin-esterase (HE) gene. It contains the entire 3′ end of the MHV-A59 genome downstream to the HE gene. The S gene open reading frame (ORF) sequences of pMH54 are identical to those of our wild-type strain MHV-A59. In addition, silent nucleotide substitutions were made at codons 12 and 13 of the S gene, generating an *Avr*II site. An *Sbf*I site was created 11 bp downstream of the termination codon of the S gene ORF (19). The *Avr*II and *Sbf*I sites were useful for introducing different S genes into the background of pMH54 (40).

To generate a plasmid containing the MHV-2 S gene, we first cloned the MHV-2 S gene into the pGEM-T$^{(a)}$ vector. MHV-2 genomic RNA was extracted from cytoplasmic RNA from infected L2 fibroblasts, and the 4,083-bp S gene was amplified using two synthetic primers, SG1F and SG1R (Table 1). The SG1F primer was used to introduce an *Avr*II restriction site immediately after the signal sequence of the S gene. The SG1R primer was used to introduce an *Sbf*I restriction site 11 bp downstream of the stop codon in the S gene. The 4,083-bp PCR fragment was gel purified, ligated into the pGEM-T$^{(a)}$ vector between the T7 and SP6 RNA polymerase promoters, and then cloned. Restriction digestion analysis of the insert was used to select positive clones, and cDNA sequencing was used to verify the S gene insert. We then removed the MHV-2 S gene from the pGEM-T$^{(a)}$ vector by digestion with *Avr*II and *Sbf*I and gel purified and subcloned it into the corresponding site in pMH54 following *Avr*II and *Sbf*I restriction site enzyme digestion, dephosphorylation, and gel purification of pMH54. The new plasmid was named pMHV2. We sequenced the S gene portion of it, in order to verify that it contained the exact sequence of the MHV-2 S gene.

Targeted RNA recombination. Targeted RNA recombination of the S gene was carried out between the Alb4 virus and synthetic capped RNAs transcribed from pMHV2 as previously described (34, 38). MHV-2 S gene recombinant viruses were selected by antibody neutralization treatment for 2 h at room temperature. The released viruses were treated with A2.1 and A2.3, anti-S monoclonal antibodies (obtained from John Fleming) that are specific for the S protein of MHV-A59. The antibody treatment neutralized the parent virus Alb4 and MHV-A59 but not MHV-2 or recombinant viruses containing the S gene derived from MHV-2. Viruses were then identified by plaque assays based on the selection of viruses with small plaques. MHV-2 produces syncytium-negative, small plaques in L2 cell cultures at 37°C. Putative recombinant viruses were identified by the presence of *Avr*II and *Sbf*I restriction sites following digestion analysis. Selected recombinants were plaque purified two more times, and viral stocks were prepared in 17Cl-1 cells. The identity of the S gene of selected recombinant viruses and the absence of mutations in the S gene were confirmed by sequence analysis.

Genome sequencing. For sequencing of the MHV-2 S gene in the various constructs, oligonucleotide primers were designed based on a recent sequence analysis of the MHV-2 genome (Das Sarma et al., submitted). Reverse transcriptase (RT) PCR amplification was carried out using cytoplasmic RNAs extracted from virus-infected L2 cell monolayers as templates. The oligonucleotides listed in Table 1 were used for amplification as specified in each experiment. Plasmid cDNAs and double-stranded PCR products were gel purified and analyzed by automated sequencing using the *Taq* dye terminator procedure from a DyeDeoxy Terminator cycle sequencing kit (Applied Biosystems). The primers used for amplification were also used for sequencing, and each fragment was sequenced in both directions.

Infection of mice. All animal experiments used 4-week-old, virus-free C57BL/6 mice (Jackson Laboratories, Bar Harbor, Maine). Viruses were diluted into phosphate-buffered saline (PBS) containing 0.75% bovine serum albumin. Mice were anesthetized with methoxyflurane (Methofane; Pittman-Moore, Mundelein, Ill.). For intracerebral (i.c.) injection, 25 μl of diluted virus was injected into the left cerebral hemisphere. Mock-infected controls were injected similarly with an uninfected L2 cell lysate at a similar dilution.

Virulence and virus titers in mice. Virulence was assessed by calculating the lethal dose that killed 50% of the mice (LD_{50}). Mice were injected i.c. with serial 10-fold dilutions of viruses (five mice per dilution). Signs of disease or death were monitored on a daily basis up to 21 days postinfection. LD_{50} values were calculated by the Reed-Muench method (41).

For measurement of virus titers in the liver and brain, mice were sacrificed at selected times postinfection (1, 3, 5, 7, 9, and 11 days postinfection) and perfused with 5 ml of sterile PBS. Brains and livers were removed aseptically and separately placed directly into 1 ml of isotonic saline with 0.167% gelatin (gel saline). All organs were stored at −80°C until virus titers were determined. Organs were homogenized, and virus titers were determined by plaque assays on L2 cell monolayers as previously described (26).

Histologic analysis. For analysis of organ pathology, mice were infected i.c., sacrificed at various times, and perfused with 5 ml of saline. Brains and livers were removed. One half of the brain and a portion of the liver were fixed in 10% phosphate-buffered formalin, and the rest of the brain and a portion of the liver were used for the evaluation of virus titers. Formalin-fixed tissues were embedded in paraffin, sectioned, and stained with hematoxylin and eosin (H&E). H&E-stained sections were used for pathological evaluation by light microscopy (24, 26). Slides were coded and read in a blinded fashion.

For assessment of demyelination, mice were infected i.c. with 5 PFU per mouse, with 10 mice per virus. At 30 days postinfection, infected mice underwent perfusion with PBS, followed by perfusion with 10% phosphate-buffered formalin. Brains and spinal cords were removed, and tissues were embedded in paraffin and sectioned for staining with Luxol fast blue to detect plaques of demyelination. Demyelination was quantified by examining one spinal cord section (four quadrants) from each of five or six levels of spinal cord for each mouse; thus, approximately 200 quadrants were examined for each dose of virus. Slides were coded and read in a blinded fashion (26, 35).

Immunohistochemical analysis. Formalin-fixed, paraffin-embedded tissue samples were deparaffinized, rehydrated through graded alcohols, and permeabilized in 0.2% Triton X-100–PBS for 15 min. Tissue was then incubated with the primary antibody (polyclonal rabbit anti-MHV; 1:100 dilution) at 37°C for 1 h, and isotype-matched negative controls were used at similar concentrations. Tissue sections with each control antibody were used in each experiment. An UltraProbe universal immunostaining kit (Biomeda Corp., Foster City, Calif.), which uses an avidin-biotin complex with alkaline phosphatase as the marker enzyme, was used in all experiments. The kit contains fast red-naphthol phosphate as the substrate-chromogen reagent. The kit was used with a MicroProbe system (Fisher Scientific, Pittsburgh, Pa.) and with capillary gap technology as previously described (13). Ten percent FBS was added to the secondary antibody as a blocking reagent against nonspecific binding. The slides were covered with Crystal/Mount (Biomeda).

Analysis of viral persistence. Four-week-old C57BL/6 mice were infected i.c. with the following viruses: 1,000 PFU of MHV-A59, 1,000 PFU of MHV-2, 2,500 PFU of wtR13, 300 PFU of Penn97-1, 5 PFU of Penn98-1, and 5 PFU of Penn98-2. The doses of 1,000 PFU of MHV-A59 (0.25 LD_{50}) and 2,500 PFU of wtR13 (0.36 LD_{50}) were known to produce sufficient demyelination. The other viruses were given at doses of 1 LD_{50} or higher to ascertain that substantial pathology would be produced in the mice in the event that persistence was not detected. Control mice were injected with uninfected cell lysate. Five mice per virus per time point were analyzed independently, with similar results (see Fig. 6 for a representative experiment).

Mice were sacrificed by an overdose of methoxyflurane and perfused intracardially with diethyl pyrocarbonate-treated PBS at 5 days postinfection (peak of acute infection) and at 30 days postinfection (peak of chronic demyelination). Organs (liver, brain, and spinal cord) were removed, snap-frozen in liquid nitrogen, ground, and homogenized to a fine powder under liquid nitrogen. RNA was isolated with an RNeasy Mini kit (Qiagen, Chatsworth, Calif.) and quantified by optical density measurement at 260 nm. Equal amounts of total tissue RNA from the samples were reverse transcribed with the SuperScript preamplification system of the first-strand cDNA synthesis kit (GIBCO BRL), and amplification was carried out by PCR. A pair of oligonucleotide primers, IZJ5 (5′-GCTCCAAC AGTTGGTGCC-3′) and IZJ6 (5′-ACGTAGGACCTTGCTAACTTC-3′) was designed for PCR amplification from the most conserved region of the N gene and the 3′ untranslated region. The reaction consisted of 3 min of denaturation at 94°C, 1 min of denaturation at 94°C, 45 s of annealing at 55°C, and 2 min of

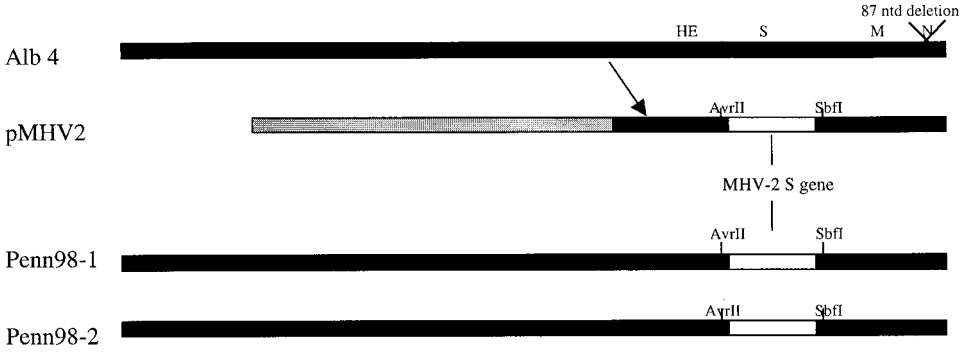

FIG. 1. Schematic diagram of targeted recombination performed in this study. Recombination occurred between Alb4 and a synthetic RNA transcribed from vector pMHV2, in which the S gene of MHV-A59 was replaced with the S gene of MHV-2. Infection of Alb4 simultaneous with transfection with pMHV2 RNA resulted in the generation of two recombinant viruses, Penn98-1 and Penn98-2, which contained the MHV-2 S gene flanked by MHV-A59 sequences (as confirmed by DNA sequencing) and the inserted *Avr*II and *Sbf*I restriction sites. Since both restriction sites derived from pMHV2 were present in the recombinant viruses, recombination must have occurred 5′ to the S gene. Black bars represent sequences derived from MHV-A59; white bars represent sequences derived from MHV-2; and gray bars represent plasmid sequences. ntd, nucleotide; M, membrane protein gene.

extension at 65°C. After 30 cycles, the final products were extended for 5 min at 72°C. The resulting amplified fragment of 601 bp was analyzed by 1.2% agarose gel electrophoresis. A second RT-PCR was performed on each sample with a second pair of N gene primers: M3 (5′-CACATTAGAGTCATCTTCTA-3′) and M4 (5′-GAAGTAGATAATGTAAGCGT-3′) (18).

RESULTS

Selection of viruses with recombinant S genes. Targeted recombination was carried out between synthetic capped RNAs transcribed from pMHV2 and the recipient virus Alb4, according to the scheme depicted in Fig. 1. Recombinant viruses, containing the MHV-2-derived S gene, were selected based on the presence of small plaques and following neutralization by the MHV-A59 S protein-specific monoclonal antibodies A2.1 and A2.3. The viruses were further plaque purified twice and analyzed for the successful repair of the Alb4 deletion. RT-PCR was carried out with primers IZJ5 and IZJ6 (Table 1), which amplified a 602-nucleotide region surrounding the 87-nucleotide N gene deletion of Alb4. The PCR-amplified product derived from Alb4 was shorter than that derived from wild-type MHV-A59; thus, recombinant viruses in which the deletion was repaired had a fragment of the same length as that amplified from wild-type virus MHV-A59 (Fig. 2A). Small-plaque viruses with larger PCR fragments were putative MHV-2 S gene recombinant viruses.

The putative recombinants were then screened for the presence of the *Avr*II and *Sbf*I restriction sites. An 868-nucleotide fragment surrounding the *Avr*II site was amplified from the genomes of all the recombinant viruses, wild-type MHV-A59, and Alb4 using primers FIJ79 and MHV-2S1R. The amplified products were digested with *Avr*II, which produced two bands of 366 and 502 bp in S recombinants but not in wild-type MHV-A59 or Alb4 (Fig. 2B). Similarly, a 1,313-nucleotide fragment surrounding the *Sbf*I site was amplified using primers Penn11F and RIJ84. Digestion with *Sbf*I generated two fragments (498 and 815 nucleotides) in S recombinants (Fig. 2C).

The S gene of recombinant viruses was sequenced using three PCR-amplified overlapping DNA fragments. One fragment was produced using primers FIJ79 and MHV-2S1R, a second one was produced using primers SG1F and SG1R, and the third was generated using primers Penn11F and RIJ84 (Table 1). The presence of the entire MHV-2 S gene with flanking regions identical to those in MHV-A59 was verified in two of the putative recombinant viruses, RC2 and RC4, which were then designated Penn98-1 and Penn98-2.

Replication and pathogenesis of chimeric viruses. The virulence of the recombinant viruses compared to that of the parental viruses was determined by LD_{50} experiments. LD_{50} experiments revealed that the virulence of both Penn98-1 and Penn98-2 (LD_{50} of each, 5 PFU) was higher than that of both parental viruses (LD_{50}s of MHV-A59 and wtR13 [40], 4,000 and 6,800 PFU, respectively) but was closer to that of MHV-2 (LD_{50}, 200 PFU). The Alb4 *ts* mutant virus was nonpathogenic in mice. To analyze the pathogenesis of the new recombinant viruses in mice, we injected mice i.c. with Penn98-1 (5 PFU = 1 LD_{50}), Penn98-2 (5 PFU = 1 LD_{50}), and wtR13 (2,500 PFU = 0.36 LD_{50}). Penn98-1 and Penn98-2 replicated efficiently in both brain and liver (Fig. 3). Liver titers of these viruses were higher than brain titers. The kinetics of replication were similar to those of MHV-2 (Das Sarma et al., submitted), suggesting that the S gene contains determinants of virulence and hepatotropism.

Brain and liver sections from animals infected i.c. with wild-type MHV-A59, wild-type MHV-2, wtR13, Penn98-1, and Penn98-2 were stained with H&E and analyzed by light microscopy. Histopathologic studies revealed that Penn98-1 and Penn98-2 produced acute meningoencephalitis similar to that caused by MHV-A59. Brain pathology consisted of focal acute encephalitis, characterized by inflammatory infiltrates of mononuclear cells (predominantly lymphocytes), microglial proliferation, microglial nodules, and neuronophagia. Areas of involvement included the regions of the brain typically susceptible to MHV-A59 infection (24). Liver pathology consisting of moderate to severe hepatitis following Penn98-1 and Penn98-2 infection was characterized by multiple foci of necrosis throughout the liver. Each area of necrosis consisted of degenerating hepatocytes, polymorphonuclear and lymphocytic inflammatory infiltrates, and cellular debris. The extent and distribution of the hepatitis caused by 5 PFU each of Penn98-1 and Penn98-2 were similar to the hepatic changes produced by 1,000 PFU of MHV-2 and more severe than the changes produced by 5,000 PFU of MHV-A59.

Immunohistochemical analysis of viral antigen was done on tissue sections obtained from mice during acute infection with the recombinant viruses (Penn98-1 and Penn98-2), and the results were compared to those for sections obtained from mice infected with MHV-A59 and MHV-2. In MHV-A59-infected mice, viral antigen was distributed in focal areas of the brain parenchyma, concomitant with the distribution of inflammatory infiltrates, as previously described (24, 29). In MHV-

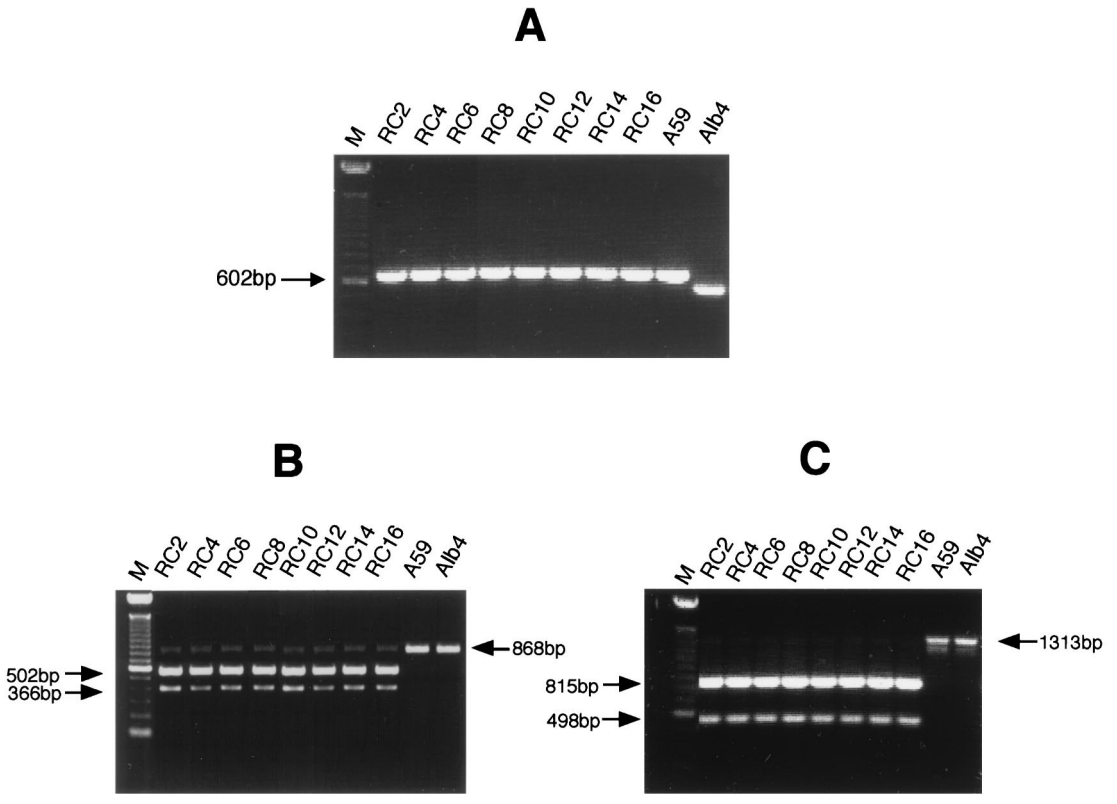

FIG. 2. RT-PCR analysis of putative recombinant viruses (RC2 to RC16). Following characterization and sequencing of the S gene region, the putative recombinant viruses RC2 and RC4 were later designated Penn98-1 and Penn98-2, respectively. (A) A 602-nucleotide region surrounding the Alb4 deletion was amplified with primers IZJ5 and IZJ6 from the genomic RNAs of putative recombinants as well as Alb4 and wild-type MHV-A59. The faster electrophoretic mobility of Alb4 corresponds to the deletion in the N gene, which does not exist in MHV-A59 and which has been repaired in all of the putative recombinant viruses tested. Lane M, size markers. (B) An 868-nucleotide fragment surrounding the *Avr*II restriction site was amplified from the genomes of putative recombinants, wild-type MHV-A59, and Alb4 using primers FIJ79 and MHV-2S1R and was digested with *Avr*II prior to electrophoresis. Undigested Alb4 and MHV-A59 are in contrast to the digested recombinant viruses, which contain the *Avr*II restriction site. (C) A 1,313-nucleotide fragment surrounding the *Sbf*I restriction site was amplified from the genomes of putative recombinant viruses, wild-type MHV-A59, and Alb4 using Penn11F and RIJ84 and was digested with *Sbf*I prior to electrophoresis. The digestion of the recombinant viruses with *Sbf*I indicates the existence of this restriction site in all of the putative recombinant viruses, in contrast to Alb4 and MHV-A59, which do not contain this restriction site.

2-infected mice, viral antigen was detected in the meninges, choroid plexus, and ependymal cells. No viral antigen was detected in neurons, and the involvement of glial cells was minimal and restricted to the subependymal location. In Penn98-1- and Penn98-2-infected mice, the distribution of viral antigen was similar to that seen with MHV-A59 infection (Fig. 4).

Demyelination in mice infected with S gene recombinant viruses. Previous studies revealed that i.c. infection of 4-week-old mice with MHV-A59 produced chronic demyelination, which could be best demonstrated in spinal cord sections at 30 days postinfection (26). Infection with MHV-2 did not produce demyelination (Das Sarma et al., submitted). To test the effect of the S gene on demyelination, we examined the ability of recombinant viruses Penn98-1 and Penn98-2 to induce demyelination compared to that of wild-type recombinant wtR13 and wild-type MHV-A59 and MHV-2. Penn98-1 and Penn98-2 did not produce demyelination in any of the seven mice injected with each virus. Like wild-type MHV-A59, wild-type recombinant wtR13, containing an S gene derived from MHV-A59, produced demyelination in 100% of the mice (five of five) (Fig. 5). All three recombinant viruses (wtR13, Penn98-1, and Penn98-2) were given at the same dose (5 PFU). The recombinant wtR13 produced larger demyelinating lesions when given at 2,500 PFU than when given at 5 PFU, but with both doses of virus, 100% of the mice were affected.

Viral persistence. In order to investigate whether differences in the abilities of viruses to cause demyelination were associated with differences in viral persistence, we amplified viral RNA from livers, brains, and spinal cords of mice infected with demyelinating and nondemyelinating viruses. As shown in Fig. 6, during the acute phase of infection, PCR products of the correct band size (601 bp), consistent with MHV RNA, were detected at 5 days postinfection in all mice infected with each of the viruses. Viral RNA was detected in all three anatomic locations examined (liver, brain, and spinal cord). However, at 30 days postinfection, PCR products corresponding to viral RNA were detected only in the MHV-A59-infected spinal cords and not in the livers or brains of the same mice. No PCR products were detected in the livers, brains, or spinal cords of mice infected with MHV-2 or another nondemyelinating virus, Penn97-1, or in organs of control uninfected mice. With a second pair of primers, RT-PCR amplified a fragment of the predicted size of 147 bp only in the sample of MHV-A59-infected spinal cord and not in the liver or brain of the same mouse. The spinal cord had the most abundant viral transcripts during the chronic phase. This result is consistent with previous reports suggesting that the spinal cord is the major site of viral persistence during chronic infection with JHM and MHV-A59 (26, 39). Mice infected with the nondemyelinating viruses

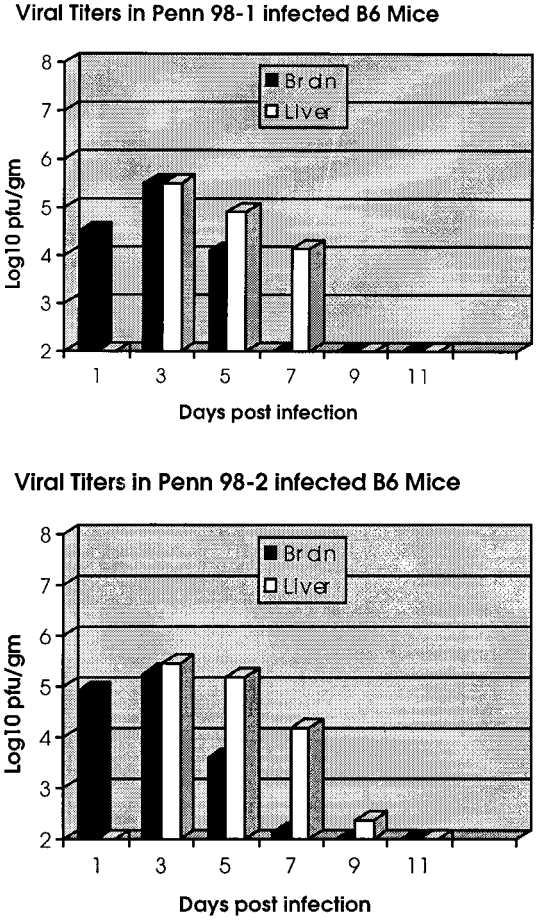

FIG. 3. Viral replication in the brains and livers of mice following i.c. injection with 5 PFU each of Penn98-1 and Penn98-2. Each time point represents the mean titer for two or three mice. Titers are expressed as $\log_{10}$ PFU per gram of tissue.

MHV-2 and Penn97-1 and uninfected controls had negative results.

To study the effect of the S gene on viral persistence, we studied infection of mice with the newly constructed recombinant viruses Penn98-1 and Penn98-2. As a control, we used wtR13, in which the S gene of MHV-A59 was reintroduced into an MHV-A59 background. Following infection with Penn98-1 and Penn98-2, viral RNA was detected in the livers and brains of the mice during the acute phase and in the spinal cords of the mice at 30 days postinfection. Similar RNA patterns were found in mice infected with wtR13 and MHV-A59. Thus, Penn-98-1 and Penn98-2 produced chronic persistent infection of the spinal cord but did not produce demyelination.

DISCUSSION

Because of the lack of an infectious clone that could be genetically manipulated, the examination of genomic control of biologic properties of coronaviruses relied, until recently, on indirect studies characterizing mutants, variants, and recombinant viruses. Recently, the technique of targeted recombination created new opportunities for the investigation of genomic determinants of biologic properties. Mutations in the 3′ end and even the exchange of complete genes became feasible. One of the most significant biologic properties of coronaviruses is the ability of some strains to persist and produce chronic inflammatory demyelination, similar to that found in MS. Information about the mechanism of this phenomenon may be useful for understanding MS, since there is strong epidemiological evidence that the immune-mediated pathology in MS may be triggered or initiated by viral infections. Thus, we began to explore the molecular determinants of demyelination in MHV-induced demyelination.

We produced two independently constructed recombinant viruses containing an S gene derived from the nondemyelinating, nonpersistent virus MHV-2. The two viruses had identical phenotypes and were able to produce encephalitis (like that caused by MHV-A59) and hepatitis (like that caused by both parental viruses) but were unable to produce demyelination similar to that caused by MHV-2. In order to rule out any possible effect of the procedure itself or mutation in the recipient virus (Alb4) used for the recombination procedure on the phenotype of the viruses, a control recombinant virus was used in parallel. The control virus (wtR13), in which an MHV-A59 S gene was reintroduced into the genome of MHV-A59, was selected using the same procedure as that used for the two recombinant viruses with the MHV-2 S genes. Control virus wtR13, as expected, had the same phenotype as wild-type MHV-A59. The inability of the viruses with an MHV-2 S gene to demyelinate suggests that the S gene may contain determi-

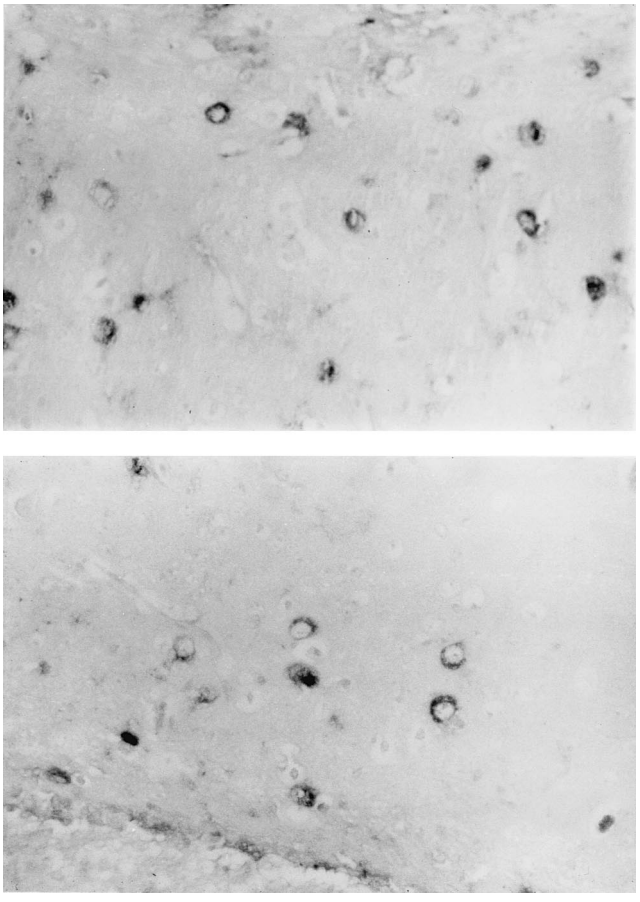

FIG. 4. Immunohistochemical detection of viral antigen in brain sections 5 days postinfection using rabbit anti-MHV polyclonal antibodies. (Top) Section from a Penn98-1-infected brain showing antigen detection in numerous neurons and glial cells in an area of acute encephalitis similar to that caused by MHV-A59. (Bottom) Section from a Penn98-2-infected brain showing similar antigen detection. Alkaline phosphatase was the marker enzyme; fast red-naphthol phosphate was the substrate-chromogen reagent; magnification, ×148.

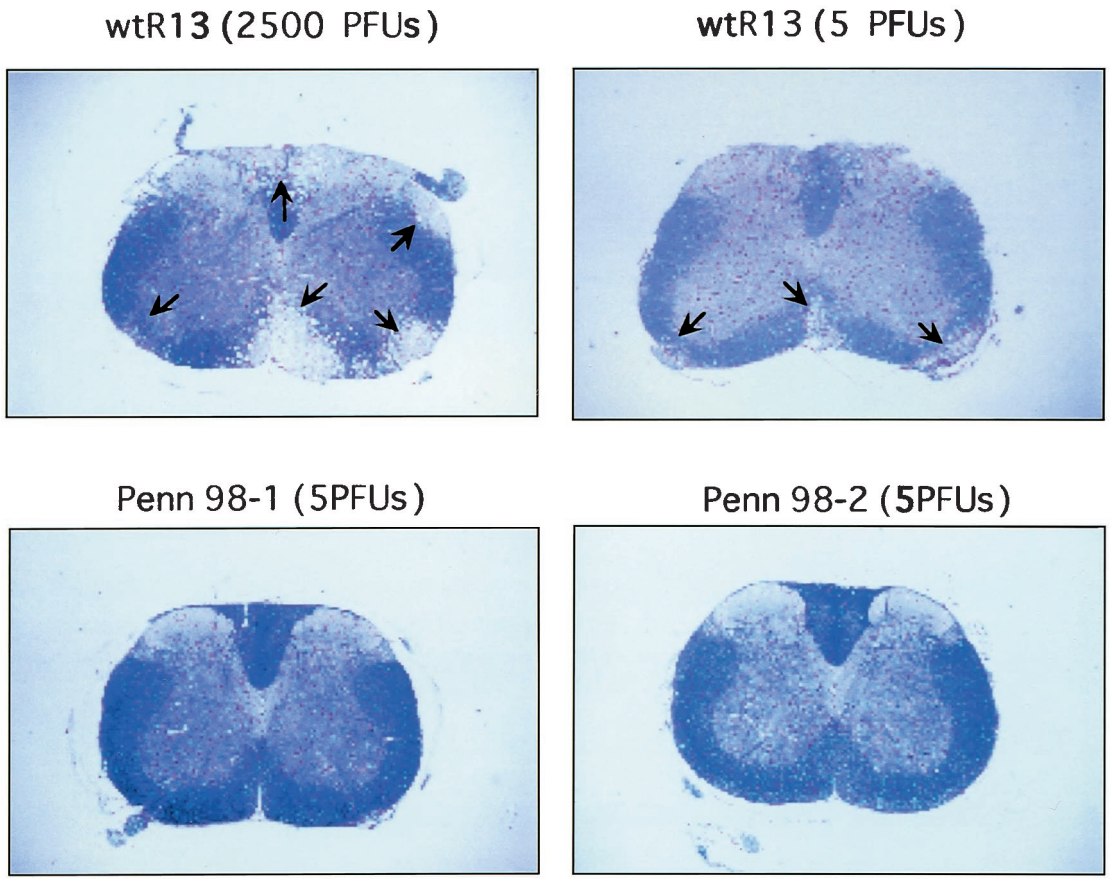

FIG. 5. Analysis of demyelination induced by recombinant viruses. Spinal cord sections were obtained from mice infected with different recombinant viruses and sacrificed 30 days after infection; the sections were stained with Luxol fast blue for myelin. Infection with wtR13 at 2,500 PFU resulted in extensive demyelination. Similar but smaller demyelinating lesions were seen in all mice infected with 5 PFU of wtR13. In contrast, all five mice infected with 5 PFU of Penn98-1 and all five mice infected with 5 PFU of Penn98-2 showed normal spinal cords at multiple levels tested.

nants of demyelination which are independent of the molecular determinants of acute encephalitis and viral persistence. Examining the phenotype of a recombinant virus with an S gene derived from MHV-A59 in an MHV-2 background would obviously further strengthen this statement. However, such recombination is not possible at the present time.

Penn98-1 and Penn98-2 both produce acute encephalitis, unlike MHV-2, which does not cause encephalitis or demyelination. Encephalitis caused by these two viruses is associated with a viral antigen distribution similar to that of MHV-A59, as shown here by immunohistochemical studies. This result suggests that although the pathologic process of encephalitis may be a prerequisite for demyelination, it is not by itself sufficient to induce demyelination, and additional determinants or factors are necessary for the induction of demyelination. This observation also suggests that important determinants of encephalitis exist outside of the S gene.

The biologic property of viral persistence is essentially the failure of the immune system to clear virus from infected organs, mainly the central nervous system. Viral persistence has been demonstrated in infections with all of the neurotropic demyelinating strains of MHV, including MHV-A59 and JHM (15, 25, 39). In most cases, only viral RNA is detectable in the chronic persistent state, but this finding may reflect only the higher sensitivity of the methods used for the detection of viral RNA than for the detection of infectious viral titers and viral antigens. Viral persistence appears to be an important factor and may even be a prerequisite for MHV-induced demyelination during chronic immune-mediated demyelination. However, MHV-induced demyelination during an acute infection may involve a different mechanism, perhaps even a direct cytolytic effect of the virus on oligodendrocytes. In the present study, we found that MHV strains that do not persist, such as MHV-2 and Penn97-1, also do not demyelinate. However, the persistence-positive, demyelination-negative, phenotype of Penn98-1 and Penn98-2 indicates for the first time that viral persistence per se is insufficient to induce demyelination. However, viral persistence may be necessary for the development of demyelination, perhaps by providing a continuous trigger for immune-mediated myelin destruction. An alternative explanation for the phenotype of Penn98-1 and Penn98-2 is that viral persistence in mice infected with these viruses may occur in neuronal cells of the gray matter, while persistence in MHV-A59-infected mice occurs in the white matter. Additional factors independent of persistence may be necessary for the development of demyelination in mice containing persistent virus. Further studies in our laboratory are under way to determine the nature of these additional factors and the precise relationship between viral persistence and demyelination.

The exchange of the S gene between MHV-2 and MHV-A59 also produced a more virulent virus. A dose of 5 PFU was sufficient to produce hepatitis and encephalitis to an extent similar to or greater than that seen with 1,000 to 5,000 PFU of wild-type parental viruses MHV-2 and MHV-A59. This finding

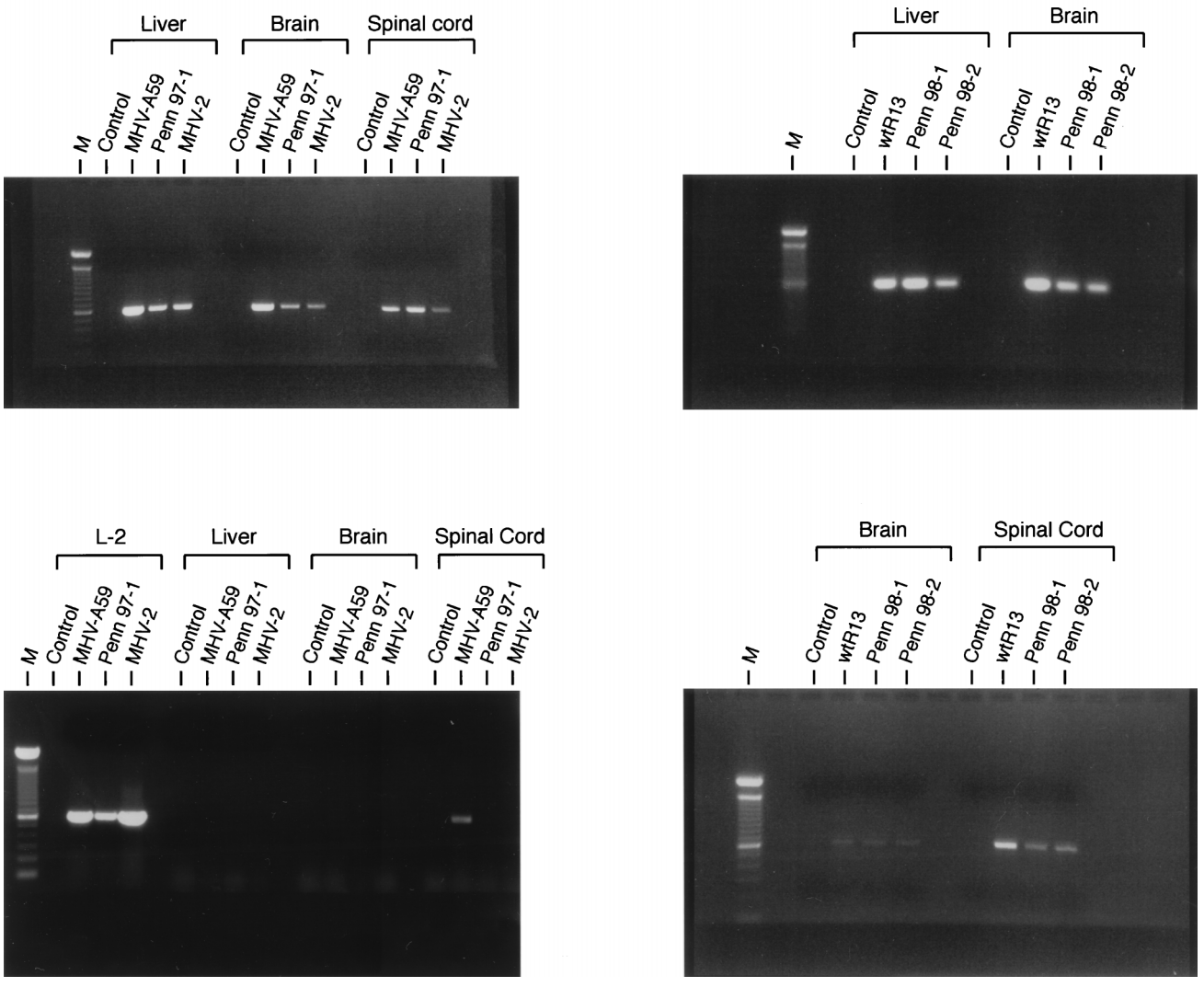

FIG. 6. Analysis of viral persistence by RT-PCR amplification with MHV-specific primers, which amplify N gene sequences conserved in all sampled viruses. Mice were sacrificed during acute disease at 5 days postinfection (top panels) or during chronic demyelinating disease at 30 days postinfection (bottom panels). Infection and mock infection of L2 fibroblast cells were used as positive and negative controls, respectively (bottom left panel). Viruses were detected in livers, brains, and spinal cords of mice during acute infection. A spinal cord signal was detected in MHV-A59-, Penn98-1-, and Penn98-2-infected mice during chronic infection but not in MHV-2- and Penn98-1-infected mice. Lanes M, size markers.

also provides further support for the observation that molecular determinants of MHV virulence are present within the S gene (40). However, determinants outside the S gene may also influence virulence. Certain interactions between different parts of the viral genome (for instance, the S gene and parts of gene 1) may account for the enhancement of viral virulence. This observation also supports the idea that homologous RNA recombination may be important for the evolution of more virulent coronaviruses or RNA viruses in general, as previously postulated (20, 21).

In conclusion, the present report provides direct evidence by targeted RNA recombination that the S gene of MHV controls certain molecular determinants of demyelination. Demyelination may depend on the integrity of other, non-S gene determinants within the viral genome. The findings presented here pave the way for further studies to investigate in more detail the potential role of the viral envelope S glycoproteins in autoimmunity and demyelination. These studies are potentially relevant to other forms of demyelination, including MS.

ACKNOWLEDGMENTS

This work was supported in part by National Multiple Sclerosis Society grant RG-2615 and PHS grant NS30606.

We thank Vahe Bedian and the staff of the DNA Sequencing Facility at the University of Pennsylvania for assistance with viral sequencing, Paul Masters for the gifts of pMH54 and Alb4 virus, John Fleming for the gift of anti-S protein monoclonal antibodies, and Elsa Aglow for histology expertise.

REFERENCES

1. **Allen, I., and B. Brankin.** 1993. Pathogenesis of multiple sclerosis—the immune diathesis and the role of viruses. J. Neuropathol. Exp. Neurol. **52:** 95–105.
2. **Anderson, D. W., J. H. Ellenberg, C. M. Leventhal, S. C. Reingold, M. Rodriguez, and D. H. Silberberg.** 1992. Revised estimate of the prevalence of multiple sclerosis in the United States. Ann. Neurol. **31:**333–336.
3. **Buchmeier, M. J., H. A. Lewicki, P. J. Talbot, and R. L. Knobler.** 1984. Murine hepatitis virus-4 (strain JHM)-induced neurologic disease is modulated in vivo by monoclonal antibody. Virology **132:**261–270.
4. **Collins, A. R., R. L. Knobler, H. Powell, and M. J. Buchmeier.** 1982. Monoclonal antibody to murine hepatitis virus-4 (strain JHM) defines the viral

glycoprotein responsible for attachment and cell-cell fusion. Virology **119:** 358–371.
5. **Dal Canto, M. C., and S. G. Rabinowitz.** 1982. Experimental models of virus-induced demyelination of the central nervous system. Ann. Neurol. **11:** 109–127.
6. **Dalziel, R. G., P. W. Lampert, P. J. Talbot, and M. J. Buchmeier.** 1986. Site-specific alteration of murine hepatitis virus type 4 peplomer glycoprotein S results in reduced neurovirulence. J. Virol. **59:**463–471.
7. **Fischer, F., C. F. Stegen, C. R. Koetzner, and P. S. Masters.** 1997. Analysis of a recombinant mouse hepatitis virus expressing a foreign gene reveals a novel aspect of coronavirus transcription. J. Virol. **71:**5148–5160.
8. **Fleming, J. O., F. I. Wang, M. D. Trousdale, D. R. Hinton, and S. A. Stohlman.** 1993. Interaction of immune and central nervous systems: contribution of anti-viral Thy-1+ cells to demyelination induced by coronavirus JHM. Regional Immunol. **5:**37–43.
9. **Gombold, J. L., and S. R. Weiss.** 1992. Mouse hepatitis virus A59 increases steady-state levels of MHC mRNAs in primary glial cell cultures and in the murine central nervous system. Microb. Pathog. **13:**493–505.
10. **Hingley, S. T., J. L. Gombold, E. Lavi, and S. R. Weiss.** 1994. MHV-A59 fusion mutants are attenuated and display altered hepatotropism. Virology **200:**1–10.
11. **Houtman, J. J., and J. O. Fleming.** 1996. Dissociation of demyelination and viral clearance in congenitally immunodeficient mice infected with murine coronavirus JHM. J. Neurovirol. **2:**101–110.
12. **Houtman, J. J., and J. O. Fleming.** 1996. Pathogenesis of mouse hepatitis virus-induced demyelination. J. Neurovirol. **2:**361–376.
13. **Jamieson, D. J., D. Usher, D. J. Rader, and E. Lavi.** 1995. Apolipoprotein(a) deposition in atherosclerotic plaques of cerebral vessels: a potential role for endothelial cells in lesion formation. Am. J. Pathol. **147:**1567–1574.
14. **Keck, J. G., L. H. Soe, S. Makino, S. A. Stohlman, and M. M. C. Lai.** 1988. RNA recombination of murine coronavirus: recombination between fusion-positive mouse hepatitis virus A59 and fusion-negative mouse hepatitis virus 2. J. Virol. **62:**1989–1998.
15. **Knobler, R. L., P. W. Lampert, and M. B. A. Oldstone.** 1982. Virus persistence and recurring demyelination produced by a temperature sensitive mutant of MHV-4. Nature **298:**279–280.
16. **Knobler, R. L., L. A. Tunison, P. W. Lampert, and M. B. A. Oldstone.** 1982. Selected mutants of mouse hepatitis virus type 4 (JHM strain) induce different CNS diseases. Pathobiology of disease induced by wild type and mutants ts8 and ts15 in BALB/c and SJL/J mice. Am. J. Pathol. **109:**157–168.
17. **Koetzner, C. A., M. M. Parker, C. S. Ricard, L. S. Sturman, and P. S. Masters.** 1992. Repair and mutagenesis of the genome of a deletion mutant of the coronavirus mouse hepatitis virus by targeted RNA recombination. J. Virol. **66:**1841–1848.
18. **Kunita, S., E. Terada, K. Goto, and N. Kagiyama.** 1992. Sequence analysis and molecular detection of mouse hepatitis virus using the polymerase chain reaction. Lab. Anim. Sci. **42:**593–598.
19. **Kuo, L., G.-J. Godeke, M. J. B. Raamsman, P. S. Masters, and P. J. M. Rottier.** 2000. Retargeting of coronavirus by substitution of the spike glycoprotein ectodomain: crossing the host cell species barrier. J. Virol. **74:**1393–1406.
20. **Lai, M. M. C.** 1992. RNA recombination in animal and plant viruses. Microbiol. Rev. **56:**61–79.
21. **Lai, M. M. C., R. S. Baric, S. Makino, J. G. Keck, J. Egbert, J. L. Leibowitz, and S. A. Stohlman.** 1985. Recombination between nonsegmented RNA genomes of murine coronaviruses. J. Virol. **56:**449–456.
22. **Lai, M. M. C., and D. Cavanagh.** 1997. The molecular biology of coronaviruses. Adv. Virus Res. **48:**1–100.
23. **Lai, M. M. C., and S. A. Stohlman.** 1981. Comparative analysis of RNA genomes of mouse hepatitis viruses. J. Virol. **38:**661–670.
24. **Lavi, E., S. P. Fishman, M. K. Highkin, and S. R. Weiss.** 1988. Limbic encephalitis following inhalation of murine coronavirus MHV-A59. Lab. Investig. **58:**31–36.
25. **Lavi, E., D. H. Gilden, M. K. Highkin, and S. R. Weiss.** 1984. Persistence of MHV-A59 RNA in a slow virus demyelinating infection in mice as detected by in situ hybridization. J. Virol. **51:**563–566.
26. **Lavi, E., D. H. Gilden, Z. Wroblewska, L. B. Rorke, and S. R. Weiss.** 1984. Experimental demyelination produced by the A59 strain of mouse hepatitis virus. Neurology **34:**597–603.
27. **Lavi, E., J. A. Haluskey, and P. S. Masters.** 1998. Targeted recombination between MHV-2 and MHV-A59 to study neurotropic determinants of MHV. Adv. Exp. Med. Biol. **440:**537–541.
28. **Lavi, E., L. Kuo, J. A. Haluskey, and P. S. Masters.** 1998. The pathogenesis of MHV nucleocapsid gene chimeric viruses. Adv. Exp. Med. Biol. **440:** 543–547.
29. **Lavi, E., E. M. Murray, S. Makino, S. A. Stohlman, M. M. Lai, and S. R. Weiss.** 1990. Determinants of coronavirus MHV pathogenesis are localized to 3′ portions of the genome as determined by ribonucleic acid-ribonucleic acid recombination. Lab. Investig. **62:**570–578.
30. **Lavi, E., T. Schwartz, Y. P. Jin, and L. Fu.** 1999. Nidovirus infections: experimental model systems of human neurologic diseases. J. Neuropathol. Exp. Neurol. **58:**1197–1206.
31. **Lavi, E., A. Suzumura, L. A. Lampson, R. M. Siegel, D. M. Murasko, D. H. Silberberg, and S. R. Weiss.** 1987. Expression of MHC class I genes in mouse hepatitis virus (MHV-A59) infection and in multiple sclerosis. Adv. Exp. Med. Biol. **218:**219–222.
32. **Lavi, E., A. Suzumura, E. M. Murray, D. H. Silberberg, and S. R. Weiss.** 1989. Induction of MHC class I antigens on glial cells is dependent on persistent mouse hepatitis virus infection. J. Neuroimmunol. **22:**107–111.
33. **Lavi, E., and S. R. Weiss.** 1989. Coronaviruses, p. 101–139. *In* D. H. Gilden and H. L. Lipton (ed.), Clinical and molecular aspects of neurotropic viral infections. Kluwer Academic Publishers, Boston, Mass.
34. **Leparc-Goffart, I., S. T. Hingley, M. M. Chua, J. Phillips, E. Lavi, and S. R. Weiss.** 1998. Targeted recombination within the spike gene of murine coronavirus mouse hepatitis virus A59: Q159 is a determinant of hepatotropism. J. Virol. **72:**9628–9636.
35. **Leparc-Goffart, I., S. T. Hingley, M.-M. Chua, X. Jiang, E. Lavi, and S. R. Weiss.** 1997. Altered pathogenesis phenotypes of murine coronavirus MHV-A59 are associated with a Q159L amino acid substitution in the receptor binding domain of the spike protein. Virology **239:**1–10.
36. **McIntosh, K.** 1974. Coronaviruses: a comparative review. Curr. Top. Microbiol. Immunol. **63:**80–129.
37. **Pachuk, C. J., P. J. Bredenbeek, P. W. Zoltick, W. J. M. Spaan, and S. R. Weiss.** 1989. Molecular cloning of the gene encoding the putative polymerase of mouse hepatitis coronavirus, strain A59. Virology **171:**141–148.
38. **Peng, D., C. A. Koetzner, T. McMahon, Y. Zhu, and P. S. Masters.** 1995. Construction of murine coronavirus mutants containing interspecies chimeric nucleocapsid proteins. J. Virol. **69:**5475–5484.
39. **Perlman, S., G. Jacobsen, A. L. Olson, and A. Afifi.** 1990. Identification of the spinal cord as a major site of persistence during chronic infection with a murine coronavirus. Virology **175:**418–426.
40. **Phillips, J. J., M. M. Chua, E. Lavi, and S. R. Weiss.** 1999. Pathogenesis of chimeric MHV4/MHV-A59 recombinant viruses: the murine coronavirus spike protein is a major determinant of neurovirulence. J. Virol. **73:**7752–7760.
41. **Reed, L., and H. Muench.** 1938. A simple method of estimating fifty percent end points. Am. J. Hyg. **27:**493–497.
42. **Stohlman, S. A., and L. P. Weiner.** 1981. Chronic central nervous system demyelination in mice after JHM virus infection. Neurology **31:**38–44.
43. **Suzumura, A., E. Lavi, S. Bhat, D. M. Murasko, S. R. Weiss, and D. H. Silberberg.** 1988. Induction of glial cell MHC antigen expression in neurotropic coronavirus infection: characterization of the H-2 inducing soluble factor elaborated by infected brain cells. J. Immunol. **140:**2068–2072.
44. **Suzumura, A., E. Lavi, S. R. Weiss, and D. H. Silberberg.** 1986. Coronavirus infection induces H-2 antigen expression on oligodendrocytes and astrocytes. Science **232:**991–993.
45. **Wang, F. I., S. A. Stohlman, and J. O. Fleming.** 1990. Demyelination induced by murine hepatitis virus JHM strain (MHV-4) is immunologically mediated. J. Neuroimmunol. **30:**31–41.
46. **Wege, H., S. Siddell, and V. ter Meulen.** 1982. The biology and pathogenesis of coronaviruses. Adv. Virol. Immunol. **99:**165–200.
47. **Weiner, L. P.** 1973. Pathogenesis of demyelination induced by a mouse hepatitis virus (JHM virus). Arch. Neurol. **28:**298–303.